Research Article GU J Sci 35(2): 446-462 (2022) DOI: 10.35378/gujs.826607

Gazi University

Journal of Science

http://dergipark.gov.tr/gujs

Direct Displacement Based Design for Reinforced Concrete Framed Structures with Seismic Isolation

Channabasaveshwar CHIKMATH *, Ankit SODHA, Sandip VASANWALA

Civil Engineering Department, Sardar Vallabhbhai National Institute of Technology, 395007, Surat, India

Highlights

- RC structures of four, eight and twelve storey are analyzed by Direct Displacement Based Design.
- Nonlinear time history analysis is performed for the ground motions according to fault distance.
- Seismic isolators in the form of Lead Rubber Bearing are used.

Article Info

Received: 16 Nov 2020
Accepted: 01 June 2021

Keywords

Direct displacement based design
Nonlinear time history analysis
Hysteretic damping
Lead rubber bearing

Abstract

Direct displacement-based design is a nonlinear static procedure and has to check the suitability of the method against different types of ground motions namely far field, near field forward directivity and near field fling step. The method is applied for the buildings supported on a fixed base and hysteretic isolation bearings. Seismic isolators are provided between the foundation and the superstructure to minimize the influence of ground motion on the superstructure. The method is applied for four, eight and twelve storey reinforced concrete frame structures equipped with and without seismic isolators. Lead rubber bearing is used as seismic isolators. An equivalent damping ratio, derived from the particular characteristics of buildings supported on isolation bearings, is suggested. The energy dissipation mechanism in the isolators controls the displacement of the structure within acceptable limits at the level of the isolator. The results were validated with nonlinear time history analysis and were found to be in good agreement with the Direct displacement-based design methodology for far field ground motions. The performance of the building was measured for interstorey drift ratio, time period, acceleration of top floor, base shear, isolator displacement. This is an attempt to link the direct displacement-based design of the reinforced concrete building with seismic isolators subjected to the far field, near field forward directivity, near field fling step ground motions.

1. INTRODUCTION

Damages induced in the structure after an earthquake are measured in terms of displacements, drifts, rotations which arises the concept of Displacement-based design which is more appealing than the traditional Force-based design method that uses forces and stresses as the input parameter. The displacement-based design has multi-performance levels to achieve the desired performance limit based on the type of the structure. Ductility is also as important as strength was realized in the 70's [1]. The first generation performance-based design procedures [2–5] laid the fundamental concepts of displacement-based design. The goal of SEAOC Vision 2000 is to develop the framework for procedures that lead to the design of structures of predictable seismic performance and can incorporate multiple performance objectives to achieve the stated performance levels for the given hazard levels [5]. Applied Technology Council emphasizes the use of the capacity spectrum method which involves determining the capacity and demand spectra. ATC 40 is limited to concrete buildings only. Although the capacity spectrum method is simple, the theoretical basis and physical interpretations are in a debatable stage [2]. FEMA 273 includes different performance objectives with associated ground motions. Analysis and design methods for the multi-level performance range from linear static to inelastic time history analysis. Drift limits for various lateral load resisting systems at different performance levels were proposed [3]. The FIB CEB-FIP [6] formulated the procedure for the displacement-based design of RC structures for Euro code [7].

*Corresponding author, e-mail: crchikmath@gmail.com

Direct Displacement Based Design (DDBD) is a displacement-based design method developed by Priestly [8] on reinforced concrete frame buildings. The method introduces the use of two different deformed shapes for buildings less than or equal to four storey and for buildings greater than four storey, hysteretic damping in addition to viscous damping in the procedure and an expression for higher modes in tall structures was proposed. The results were validated using time history analysis of various earthquake intensity ranges. The results obtained by the equations proposed by Priestley were in good agreement with time history analysis. Different structural systems namely moment-resisting frame, wall frame and steel braced systems with the direct displacement-based design were analyzed and validated by nonlinear time history analysis which proved that the DDBD approach was efficient [9]. Direct displacement-based design in two and three-bay reinforced concrete structures was carried out considering plastic hinge length, longitudinal reinforcement ratio in the members [10]. The expression for considering higher modes in direct displacement-based design for vertically irregular moment-resisting frames was put forward and verified with nonlinear time history analysis [11]. An effort was made to simplify the direct displacement-based design method using viscous dampers [12]. Two displacement-based methods namely direct displacement-based design and displacement-based seismic design method using damage control were applied on a twelve storeys plan irregular RC frame building [13]. The latter one gave a better result but still needs to be validated considering the different configuration of the building. A performance-based assessment tool known as Displacement-based adaptive pushover analysis was applied for concrete frame buildings varying in height [14]. Seismic performance of steel moment resisting frame was carried on four, six and storey with mass irregularity [15].

Ground motion records are of two types, based on the distance of the recording station from the fault site namely far field(>15km) and near field(<15km) [16]. Far field ground motions have large amplitude and longer duration. The directivity effect and fling-step effect are the two paramount effects associated with near-field earthquakes. In forward directivity, rupture propagation is aligned to the site and fault rupture velocity is approximately equal to the shear wave velocity of the site [17]. This results in large amplitude, long period and short duration. The permanent ground displacement due to tectonic deformations causes the fling step effect. It produces large amplitude velocity pulse. Diagrammatic representation of the far field, forward directivity and fling step is shown in Figure 1.

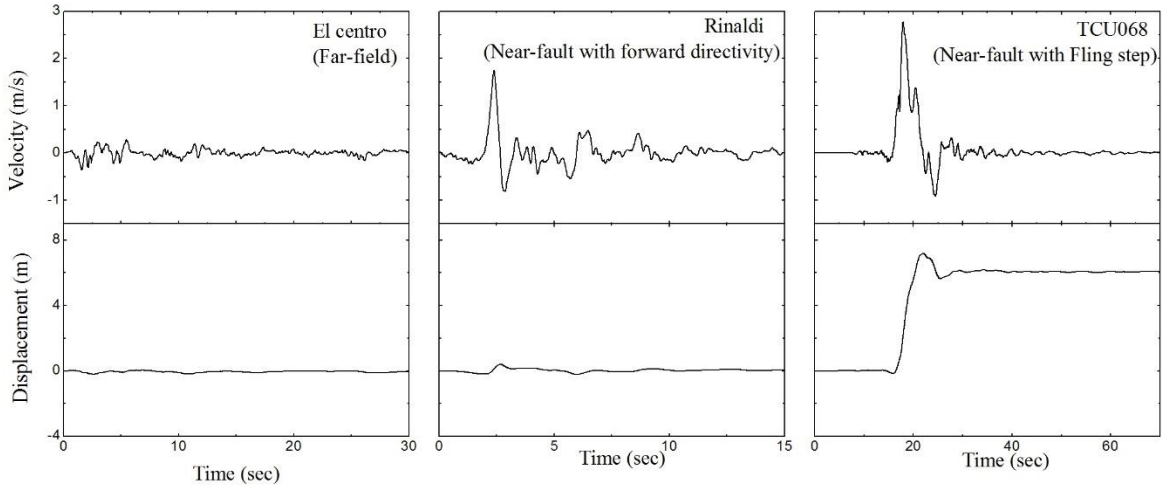

Figure 1*. Comparison of far field, forward directivity and fling step ground motions*

The seismic response of six storey and thirteen storey buildings due to fling step and forward directivity were determined [17]. Moghim et al., [18] applied direct displacement-based design for concrete buildings situated in near fault regions. Alternate to the Gutenberg-Richter model, the interrelation between the

number of earthquakes and their magnitudes was proposed by considering 4863 ground motions of magnitude 4.0 and above [19].

The term responsive index was coined to compare and achieve the stated performance levels in fixed and base-isolated structure [20]. The effect of the behaviour of the base-isolated ten storey building with and without the shear wall, yielded large peak storey drift in moment resisting frames than the shear wall building [21]. Bhandari et al., [22] worked on ten storey base-isolated RC building frame subjected to the far field, near field forward directivity and near field fling step ground motions of design base earthquake(DBE) and maximum considered earthquake(MCE) in terms of base shear, floor acceleration, interstorey drift, isolator displacement and the number of hinges formed. Lead rubber bearing was used as the isolator. Hallow rubber bearing was found more efficient when compared to solid rubber bearing since the stiffness is reduced in the former when compared to the latter [23]. Rubber bearings and dampers were found effective in reducing the damage due to earthquake on the steel liquid storage tank [24].

Although seismic base isolation and displacement-based design were developed in the 70s only, the displacement-based design with the base isolation on bridges was applied in 2008 [25] and on buildings in 2010 [26]. Cardone et al., [26] modified the direct displacement-based design developed by Priestley [8] for the different types of base-isolated frame structures.

In this work, the direct displacement-based design procedure developed by Cardone et al., [26] is applied on fixed base(FB) and base-isolated(BI) building of four, eight and twelve storey RC frame buildings considered as low-rise, medium-rise and high-rise buildings [9,27] respectively which form the major frame buildings in India located in Zone-V, medium soil of Indian seismic code [28] subjected to the far field, near field forward directivity and near field fling step ground motions. Seismic isolator in the form of Lead rubber bearing (LRB) is used. An equivalent damping ratio, derived from the particular characteristics of buildings supported on isolation bearings, is suggested. The energy dissipation mechanism in the isolators controls the displacement of the structure within acceptable limits at the level of the isolator. The mechanical properties of the isolator are derived after literature review and selected after a thorough examination of the product catalogue available on the manufacturer's website [29–32]. The performance of the buildings is measured concerning inter-storey drift ratio, roof acceleration, base shear, isolator displacement. The buildings are designed by the Indian concrete code [33].

2. PROCEDURE

In this method, a multi-degree of freedom system is represented into an equivalent single degree with effective mass m_e and effective height h_e as shown in Figure 2. K_e is the secant stiffness of the system at the ultimate displacement of this system shown in Figure 3. The procedure is as follows:

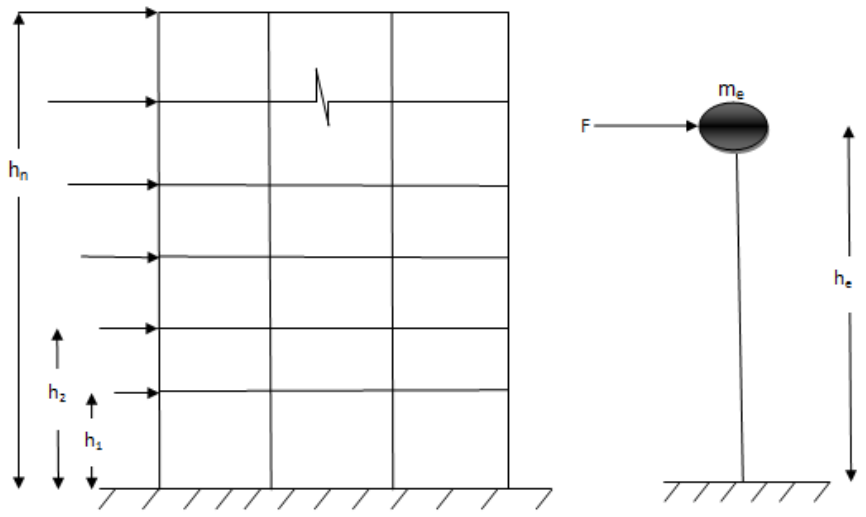

Figure 2*. Simulation of MDOF to SDOF*

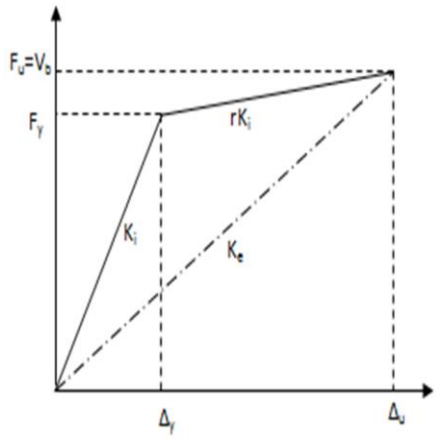

***Figure 3**. Effective stiffness*

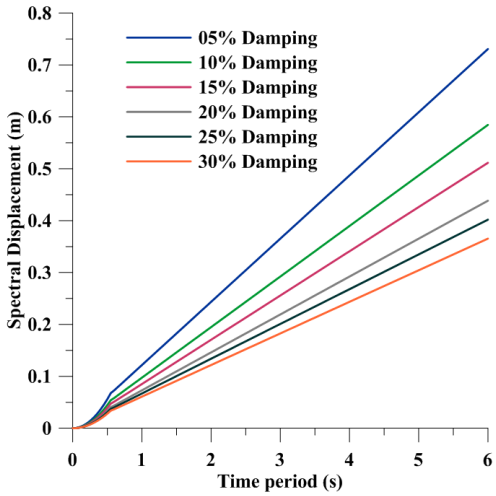

***Figure 4**. Displacement spectrum for IS 1893-2016 for Zone- V*

1. The first mode deformed shape is derived using the expression [26] given by

$$\Phi_i = \cos\left[\left(\frac{1}{I_r}\right).\left(1-\frac{h_i}{h_n}\right).\frac{\pi}{2}\right] - \cos\left[\left(\frac{1}{I_r}\right).\frac{\pi}{2}\right] \quad (1)$$

where h_i= height of i^{th} storey from the base, h_n=total height of the structure, I_r is the ratio of the effective period of vibration of seismically isolated structure to fundamental period of vibration of fixed support building. For fixed supported building, I_r=1.

2. Select the appropriate base isolator with the isolator displacement D_d and maximum interstorey drift ratio θ_d. The critical storey is the storey where the maximum interstorey drift ratio is reached. The maximum interstorey drift ratio is reached in the first storey [13] and is assumed as

$$\theta_d = 100\frac{\Delta_c}{h_c}. \quad (2)$$

3. The displacement profile [26] for the i^{th} storey of the structure is given as

$$\Delta_i = D_d + \theta_d.c_1.\Phi_i\,, \quad (3)$$

$$c_1 = \frac{h_1}{100\Phi_1}. \quad (4)$$

4. Design displacement Δ_d, effective mass m_e, the effective height h_e of equivalent SDOF system are given by Equations (5)-(7), respectively

$$\Delta_d = \frac{\sum_{i=1}^{n} m_i \Delta_i^{\,2}}{\sum_{i=1}^{n} m_i \Delta_i}, \tag{5}$$

$$m_e = \frac{\sum_{i=1}^{n} m_i \Delta_i}{\Delta_d} = \frac{[\sum_{i=1}^{n} m_i \Delta_i]^2}{\sum_{i=1}^{n} m_i \Delta_i^{\,2}}, \tag{6}$$

$$h_e = \frac{\sum_{i=1}^{n} m_i \Delta_i h_i}{\sum_{i=1}^{n} m_i \Delta_i}. \tag{7}$$

5. Since displacement, drift, ductility are the governing parameters in the displacement-based design method, design ductility can be controlled as

$$\mu_d = \frac{\theta_d}{\theta_y}, \tag{8}$$

$$\theta_y = 0.5\varepsilon_y \frac{l_b}{h_b}, \tag{9}$$

ε_y=yield strain in steel=0.2%, l_b=beam length and h_b=beam depth .

6. In addition to 5% elastic viscous damping, hysteretic damping is added to include energy dissipation by RC members during the earthquake and is known as equivalent viscous damping of the superstructure [13]

$$\xi_S = (5 + \xi_{hyst})\%,$$
$$\xi_S = 5 + 120\left(\frac{1 - \mu_d^{\,-0.5}}{\pi}\right)\%. \tag{10}$$

7. The equivalent damping ratio ξ_{eq} of base-isolated structure is the combination of damping ratios of superstructure and base isolator at their corresponding displacements given as

$$\xi_{eq} = \frac{[\xi_{IS}.D_d + \xi_S.(\Delta_D - D_d)]}{\Delta_D}. \tag{11}$$

8. The effective time period T_{eq} is established by entering the displacement spectra set shown in Figure 4 with the design displacement Δ_d and the equivalent viscous damping.

9. The equivalent stiffness K_{eq} for the design displacement of the equivalent SDOF system using

$$K_{eq} = 4\pi^2 \frac{m_e}{T_{eq}^2}. \tag{12}$$

10. The base shear is the product of equivalent stiffness K_{eq} and the design displacement Δ_d, given as

$$V_{b(DDBD)} = K_{eq}\Delta_d. \tag{13}$$

11. Distribute the base shear along the height of the building using Equation (14)

$$F_i = V_{b(DDBD)} \cdot \frac{m_i \Delta_i}{\sum_{i=1}^{n} m_i \Delta_i}. \tag{14}$$

12. The stiffness of the base isolator is given by

$$K_{IS} = \frac{V_{b(DDBD)}}{D_d}. \tag{15}$$

3. CHARACTERISTICS OF LEAD RUBBER BEARING

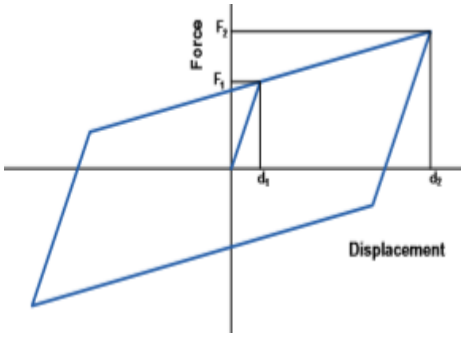

***Figure 5**. Hysteresis loop for LRB*

The hysteresis loop is typically modelled as bilinear for a lead rubber bearing isolator. The parameters F_1, d_1, F_2 and d_2 that define the bilinear curve are given by the manufacturers for each standard LRB [29–32]. The hysteretic behaviour of an LRB can also be modelled as linear, using the effective stiffness K_e and the equivalent viscous damping coefficient ξ_{IS}, which depends on the maximum displacement d_2 and the corresponding force F_2, to which refer to Figure 5.

$$K_e = \frac{F_2}{d_2}$$

$$\xi_{IS} = \frac{2}{\pi}\left[\frac{F_1}{F_2} - \frac{d_1}{d_2}\right]$$

4. CHARACTERISTICS OF GROUND MOTIONS

Ground motion data of six set each for the far field, near field forward directivity and near field fling step respectively have been selected [34]. The details of the ground motions in terms of magnitude, recording station, PGA, fling step displacement are shown in Table 1.

***Table 1**. Ground motion records*

Record Label	Earthquake	Magnitude	Station	PGA (g)	Fling Disp. (cm)
Far-field ground motions					
FF 1	1999 Chamoli	6.4	Chamoli	0.359	-
FF 2	1940 Imperial Valley	6.95	El Centro	0.313	-
FF 3	1989 Loma Prieta	6.9	Capitola	0.420	-
FF 4	1994 Northridge	6.7	Northridge-Saticoy	0.529	-
FF 5	1994 Northridge	6.7	Canoga Park	0.477	-
FF 6	1987 Superstition Hills	6.7	El Centro Imp Co. Centre	0.512	
Near-fault ground motions with forward directivity					
NFD 1	1994 Northridge	6.7	Rinaldi	0.890	-
NFD 2	1994 Northridge	6.7	Sylmar	0.730	-
NFD 3	1994 Northridge	6.7	Newhall	0.720	-
NFD 4	1979 Imperial Valley	6.4	EL Centro Array 7	0.460	-
NFD 5	1992 Landers	7.3	Lucerne Valley	0.710	-
NFD 6	1979 Imperial Valley	6.7	EL Centro Array 5	0.370	
Near-fault ground motions with fling step					
NFS1	1999 Chi Chi	7.6	TCU129_NS	0.610	67.54
NFS 2	1999 Chi Chi	7.6	TCU084_NS	0.420	59.43
NFS 3	1999 Chi Chi	7.6	TCU074 EW	0.590	174.56
NFS4	1999 Chi Chi	7.6	TCU052_NS	0.440	697.12
NFS5	1999 Chi Chi	7.6	TCU068_EW	0.500	601.84
NFS 6	1999 Kocaeli	7.4	YPT	0.23	145.79

5. BUILDING DETAILS

The plan of an RC frame building with dimensions is shown in Figure 6 for four, eight and twelve storeys respectively. The building is located in medium soil for the Bhuj area which falls under Zone-V considered an extreme zone according to the Bureau of Indian Standards [28]. The design is carried out using the Bureau of Indian Standard code [33]. The drift is limited to 2% [5,10]. Nonlinear time history analysis (NLTHA) is carried out to verify the inter-story drift ratio, acceleration of top floor, base shear, isolator displacement for six sets of each earthquake ground motions of far field, near field forward directivity and near field fling step respectively scaled to Zone-V [28] using with FB and BI. The analysis and design were carried out in MIDAS/GEN 2019 software. The live load is 3kN/m^2. External wall of 230mm thick exists. The thickness of the slab is 150mm. Characteristic strength of main steel and secondary steel are 500N/mm^2 and 415 N/mm^2 respectively. Secondary beams are 300mm in width and 450mm in depth. The dimensions of the members are as shown in Table 2. The lead rubber bearing provided is manufactured by *FIP INDUSTRIALE* [31]. The isolators were selected based on the maximum isolator displacement, a good separation of the time period for fixed and base-isolated structure and axial load coming on the columns [22,35]. Isolator properties are shown in Table 3.

Table 2*. Properties of frame building*

	Member	Floor	Width (mm)	Depth (mm)	Grade of concrete cube (N/mm^2)
4-Storey	Beam	1-4	300	600	30
	Column		550	550	
8-Storey	Beam	1-8	300	600	30
	Column		650	650	
12-Storey	Beam	1-12	300	600	30
	Column		750	750	

Table 3*. Isolator properties*

	4 Storey	8 Storey	12 Storey
Name of the isolator	LRB-S 550/200-120	LRB-S 550/200-120	LRB-S 600/204-130
Isolator Displacement D_d	0.4 m	0.4 m	0.4 m
Effective Stiffness K_{eff}	810 kN/m	810 kN/m	950 kN/m
Initial Stiffness K_1	7875 kN/m	7875 kN/m	9250 kN/m
Effective Damping ξ_{IS}	26.65%	26.65%	26.85%
Post Yield Stiffness Ratio γ	0.058	0.058	0.057
Yield Force F_y	126 kN	126 kN	148 kN
Vertical Stiffness K_v	789000 kN/m	789000 kN/m	844000 kN/m

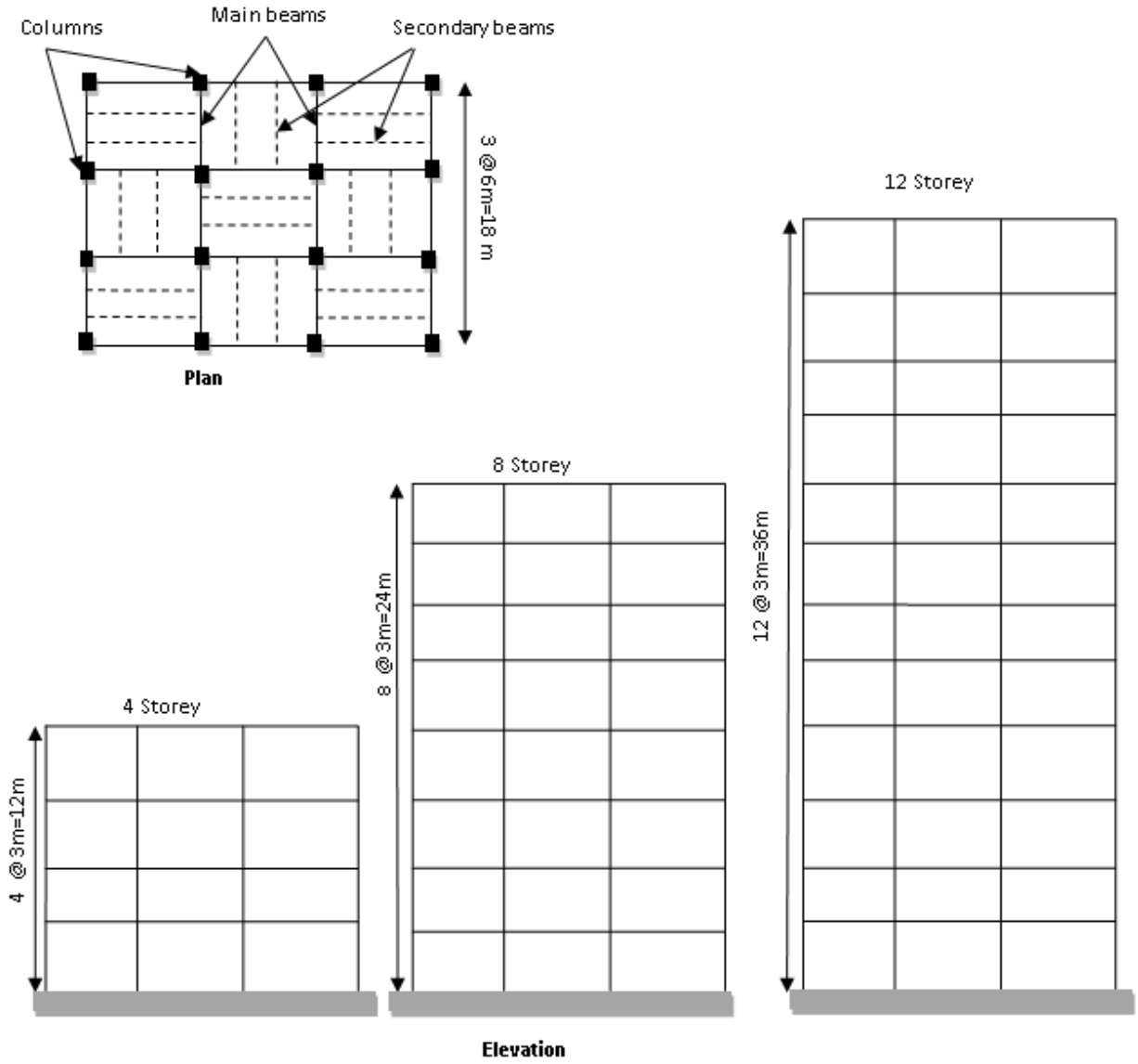

Figure 6. *Geometry of the building*

Table 4. *Results of analysis*

No of storeys	T_{eq} (s)	I_r	ξ_{eq}(%)		$V_{b(DDBD)}$ (kN)	
			BI	FB	BI	FB
4	5.30	3.39	24.70	16.19	1237	3524
8	5.70	2.43	23.11	16.19	2621	3554
12	6.08	2.05	22.17	16.19	4116	4136

Table 5. *Four storey response parameters*

Earthquake	Type of structure	Roof accel (m/s^2)	Max Drift ratio (%)	Roof disp (mm)	first floor disp (mm)	Isolator disp (mm)
FF1	FB	1.37	0.18	17.5	3.4	
	BI	1.00	0.36	42.6	27.4	16.7
	% reduction	26.96	-98.15	-143.43		
FF2	FB	2.52	0.47	44.6	8.5	
	BI	1.31	0.61	72.9	56.3	44.2
	% reduction	48.03	-27.82	-63.45		
FF3	FB	1.54	0.28	24.6	4.9	
	BI	1.04	0.34	39.2	25.2	15
	% reduction	32.60	-20.00	-59.35		
FF4	FB	1.94	0.27	24.2	4.8	
	BI	0.90	0.37	38.8	23.9	12.9
	% reduction	53.61	-34.15	-60.33		
FF5	FB	1.79	0.30	24	5.5	
	BI	1.25	0.38	51	31.2	19.7
	% reduction	30.13	-29.21	-112.50		
FF6	FB	1.79	0.28	24.7	4.9	
	BI	1.05	0.35	40	25.5	15
	% reduction	41.64	-26.51	-61.94		
NFD1	FB	1.86	0.29	25.3	6.2	
	BI	1.477	0.40	82.1	70	57.9
	% reduction	20.63	-37.50	-224.51		
NFD2	FB	2.05	0.41	38.6	7.3	
	BI	1.266	0.30	59.8	50.4	41.3
	% reduction	38.27	26.02	-54.92		
NFD3	FB	1.81	0.35	32.9	6	
	BI	1.15	0.16	46.1	41.6	36.8
	% reduction	36.63	53.85	-40.12		
NFD4	FB	1.45	0.21	21.2	4	
	BI	1.30	0.28	44.7	36.5	28.1
	% reduction	10.81	-35.48	-110.85		
NFD5	FB	1.90	0.31	23.6	5.7	
	BI	1.40	0.23	45.3	38.6	31.8
	% reduction	26.47	26.09	-91.95		
NFD6	FB	2.10	0.31	27.6	6.2	
	BI	1.27	0.31	51.9	42.6	33.4
	% reduction	39.34	2.13	-88.04		
NFS1	FB	2.01	0.29	28.1	5.6	
	BI	1.46	0.33	59.3	48.8	38.8
	% reduction	27.44	-14.94	-111.03		
NFS2	FB	2.04	0.39	32.9	7.2	
	BI	1.45	0.40	63.9	51.7	39.8
	% reduction	29.07	-0.85	-94.22		
NFS3	FB	2.10	0.22	19.2	4.1	
	BI	1.23	0.19	36.3	30.2	24.5
	% reduction	41.70	12.31	-89.06		
NFS4	FB	1.46	0.23	18.4	4.1	
	BI	1.19	0.26	38	30.2	22.4
	% reduction	18.71	-13.04	-106.52		
NFS5	FB	2.19	0.28	25.1	5.3	
	BI	1.43	0.21	48.2	41.6	35.4
	% reduction	34.81	26.19	-92.03		
NFS6	FB	2.07	0.25	19.3	4.5	
	BI	1.23	0.23	39.8	32.1	25.3
	% reduction	40.55	9.33	-106.22		

Table 6*. Eight storey response parameters*

Earthquake	Type of structure	Roof accel (m/s^2)	Max Drift ratio (%)	Roof disp (mm)	first floor disp (mm)	Isolator disp (mm)
FF1	FB	0.95	0.36	58.2	4.6	
	BI	0.70	0.24	66.6	47.2	40
	% reduction	26.15	32.71	-14.43		
FF2	FB	1.49	0.42	70.8	5.1	
	BI	0.72	0.29	101.4	78.1	69.3
	% reduction	51.61	29.60	-43.22		
FF3	FB	0.91	0.43	69.6	5.8	
	BI	0.68	0.39	81	50.9	39.2
	% reduction	25.24	10.00	-16.38		
FF4	FB	0.94	0.40	65.9	5.3	
	BI	0.69	0.29	66.7	43.8	35.2
	% reduction	25.99	28.33	-1.21		
FF5	FB	1.07	0.47	78.1	6.2	
	BI	0.74	0.37	85.9	57.1	46
	% reduction	31.18	21.28	-9.99		
FF6	FB	0.94	0.35	56.7	4.6	
	BI	0.67	0.21	59.7	37.4	31.2
	% reduction	28.32	40.38	-5.29		
NFD1	FB	1.42	0.74	121	9.9	
	BI	0.89	0.63	203.1	153.9	135.1
	% reduction	37.10	15.32	-67.85		
NFD2	FB	1.26	0.84	137.3	11.1	
	BI	1.00	0.72	256.4	199.4	177.8
	% reduction	20.62	14.29	-86.74		
NFD3	FB	1.02	0.39	65.9	5.3	
	BI	0.67	0.34	74.3	46.8	36.6
	% reduction	34.38	12.82	-12.75		
NFD4	FB	1.17	0.56	90.4	7.3	
	BI	0.79	0.41	109.3	76.9	64.5
	% reduction	32.25	25.75	-20.91		
NFD5	FB	1.06	0.37	60	5.1	
	BI	0.76	0.25	56.7	35.7	28.2
	% reduction	28.59	32.43	5.50		
NFD6	FB	1.31	0.55	91.7	7.4	
	BI	0.78	0.34	100.2	73.2	62.9
	% reduction	40.63	37.58	-9.27		
NFS1	FB	1.36	0.59	99.2	7.6	
	BI	0.89	0.47	135.1	97.6	83.6
	% reduction	34.10	21.35	-36.19		
NFS2	FB	1.20	0.62	102.7	8.3	
	BI	0.82	0.49	127	88.8	74.2
	% reduction	31.39	21.08	-23.66		
NFS3	FB	0.92	0.38	61.9	5.1	
	BI	0.68	0.33	64.5	37.9	27.9
	% reduction	26.47	13.04	-4.20		
NFS4	FB	1.11	0.45	75.5	6	
	BI	0.77	0.30	77.6	53.5	44.5
	% reduction	30.87	33.82	-2.78		
NFS5	FB	1.03	0.35	58.9	4.3	
	BI	0.76	0.29	67.8	45.1	36.5
	% reduction	26.18	18.87	-15.11		
NFS6	FB	0.99	0.49	80.3	6.3	
	BI	0.74	0.41	96.3	64	51.6
	% reduction	24.96	15.65	-19.93		

Table 7. *Twelve storey response parameters*

Earthquake	Type of structure	Roof accel (m/s^2)	Max Drift ratio (%)	Roof disp (mm)	first floor disp (mm)	Isolator disp (mm)
FF1	FB	0.64	0.38	92.4	3.6	
	BI	0.52	0.22	75.6	32.8	26.6
	% reduction	18.03	41.59	18.18		
FF2	FB	0.72	0.39	91.8	4	
	BI	0.55	0.32	89.6	45.8	36.1
	% reduction	22.82	17.09	2.40		
FF3	FB	0.78	0.65	155.1	6.4	
	BI	0.57	0.47	133.8	69.9	55.8
	% reduction	26.60	27.32	13.73		
FF4	FB	0.71	0.39	92.8	4.1	
	BI	0.59	0.27	77.7	36.5	28.3
	% reduction	16.61	29.31	16.27		
FF5	FB	0.75	0.52	129	5	
	BI	0.60	0.40	113.3	58.4	46.4
	% reduction	20.52	23.08	12.17		
FF6	FB	0.67	0.37	90.8	4	
	BI	0.56	0.28	76.8	37.8	29.5
	% reduction	16.45	25.23	15.42		
NFD1	FB	1.46	1.37	350.2	14.1	
	BI	0.85	0.86	367.6	248.9	223.1
	% reduction	41.79	37.38	-4.97		
NFD2	FB	1.58	1.64	409.9	15.8	
	BI	0.92	0.92	413.2	284.4	256.7
	% reduction	41.83	43.81	-0.81		
NFD3	FB	0.70	0.55	133.6	5.3	
	BI	0.55	0.43	122.2	63.8	50.8
	% reduction	22.00	20.73	8.53		
NFD4	FB	0.86	0.63	157.5	5.9	
	BI	0.64	0.46	140.7	76.4	62.7
	% reduction	25.25	27.89	10.67		
NFD5	FB	0.77	0.48	112.6	5.2	
	BI	0.55	0.36	91.7	44.7	33.9
	% reduction	29.40	25.00	18.56		
NFD6	FB	1.00	0.62	148.6	6	
	BI	0.65	0.37	122.8	72	60.9
	% reduction	34.77	40.64	17.36		
NFS1	FB	0.76	0.84	201.3	8.6	
	BI	0.69	0.50	207.4	123.2	108.2
	% reduction	8.79	40.48	-3.03		
NFS2	FB	0.89	0.76	185.5	8.1	
	BI	0.67	0.59	193	111.9	94.1
	% reduction	24.69	21.59	-4.04		
NFS3	FB	0.68	0.55	134	5.3	
	BI	0.55	0.43	110.5	50.4	37.5
	% reduction	19.19	22.29	17.54		
NFS4	FB	0.80	0.42	100.6	4.3	
	BI	0.64	0.25	85.1	46.5	38.9
	% reduction	19.84	39.68	15.41		
NFS5	FB	0.64	0.38	93.4	3.6	
	BI	0.60	0.28	78.9	38.6	30.2
	% reduction	6.23	26.32	15.52		
NFS6	FB	0.75	0.65	160.7	6.3	
	BI	0.60	0.50	143	73.6	58.6
	% reduction	19.71	23.47	11.01		

Table 8. *Four storey base shear ratios V_b (NLTHA)/V_b (DDBD)*

			Far field			Near field forward directivity			Near field fling step		
	$V_b^{(a)}$			$V_b^{(b)}$	(b)/(a)		$V_b^{(c)}$	(c)/(a)		$V_b^{(d)}$	(d)/(a)
BI DDBD	1237	BI Time history	FF1	942	0.76	NFD1	1541	1.25	NFS1	1372	1.11
			FF2	1088	0.88	NFD2	1428	1.15	NFS2	1481	1.20
			FF3	941	0.76	NFD3	1016	0.82	NFS3	1037	0.84
			FF4	970	0.78	NFD4	1251	1.01	NFS4	1172	0.95
			FF5	885	0.72	NFD5	1173	0.95	NFS5	1198	0.97
			FF6	943	0.76	NFD6	1268	1.02	NFS6	1232	1.00
FB DDBD	3524	FB Time history	FF1	1216	0.35	NFD1	1973	0.56	NFS1	1802	0.51
			FF2	1906	0.54	NFD2	1661	0.47	NFS2	1692	0.48
			FF3	1213	0.34	NFD3	1432	0.41	NFS3	1285	0.36
			FF4	1190	0.34	NFD4	1501	0.43	NFS4	1328	0.38
			FF5	1397	0.40	NFD5	1438	0.41	NFS5	1536	0.44
			FF6	1217	0.35	NFD6	1519	0.43	NFS6	1303	0.37

Table 9. *Eight storey base shear ratios V_b (NLTHA)/V_b (DDBD)*

			Far field			Near field forward directivity			Near field fling step		
	$V_b^{(a)}$			$V_b^{(b)}$	(b)/(a)		$V_b^{(c)}$	(c)/(a)		$V_b^{(d)}$	(d)/(a)
BI DDBD	2621	BI Time history	FF1	1724	0.66	NFD1	2769	1.06	NFS1	2277	0.87
			FF2	1835	0.70	NFD2	3120	1.19	NFS2	2259	0.86
			FF3	1973	0.75	NFD3	1852	0.71	NFS3	1782	0.68
			FF4	1743	0.66	NFD4	2148	0.82	NFS4	1797	0.69
			FF5	1980	0.76	NFD5	1674	0.64	NFS5	1737	0.66
			FF6	1722	0.66	NFD6	1930	0.74	NFS6	1927	0.74
FB DDBD	3554	FB Time history	FF1	1776	0.50	NFD1	2961	0.83	NFS1	2372	0.67
			FF2	2052	0.58	NFD2	3317	0.93	NFS2	2563	0.72
			FF3	2074	0.58	NFD3	2036	0.57	NFS3	1979	0.56
			FF4	2030	0.57	NFD4	2357	0.66	NFS4	2151	0.61
			FF5	2165	0.61	NFD5	1894	0.53	NFS5	1715	0.48
			FF6	1814	0.51	NFD6	2423	0.68	NFS6	2144	0.60

Table 10. *Twelve storey base shear ratios V_b (NLTHA)/V_b (DDBD)*

			Far field			Near field forward directivity			Near field fling step		
	$V_b^{(a)}$			$V_b^{(b)}$	(b)/(a)		$V_b^{(c)}$	(c)/(a)		$V_b^{(d)}$	(d)/(a)
BI DDBD	4095	BI Time history	FF1	2053	0.50	NFD1	4114	1.00	NFS1	2937	0.72
			FF2	2025	0.49	NFD2	4397	1.07	NFS2	2986	0.73
			FF3	2636	0.64	NFD3	2493	0.61	NFS3	2432	0.59
			FF4	2015	0.49	NFD4	2670	0.65	NFS4	1997	0.49
			FF5	2405	0.59	NFD5	2181	0.53	NFS5	1934	0.47
			FF6	2094	0.51	NFD6	2444	0.60	NFS6	2691	0.66
FB DDBD	4136	FB Time history	FF1	1712	0.41	NFD1	4767	1.15	NFS1	3329	0.81
			FF2	1980	0.48	NFD2	5406	1.31	NFS2	3224	0.78
			FF3	2705	0.65	NFD3	2327	0.56	NFS3	2395	0.58
			FF4	2186	0.53	NFD4	2649	0.64	NFS4	2190	0.53
			FF5	2420	0.59	NFD5	2501	0.60	NFS5	1671	0.40
			FF6	2045	0.49	NFD6	2809	0.68	NFS6	2606	0.63

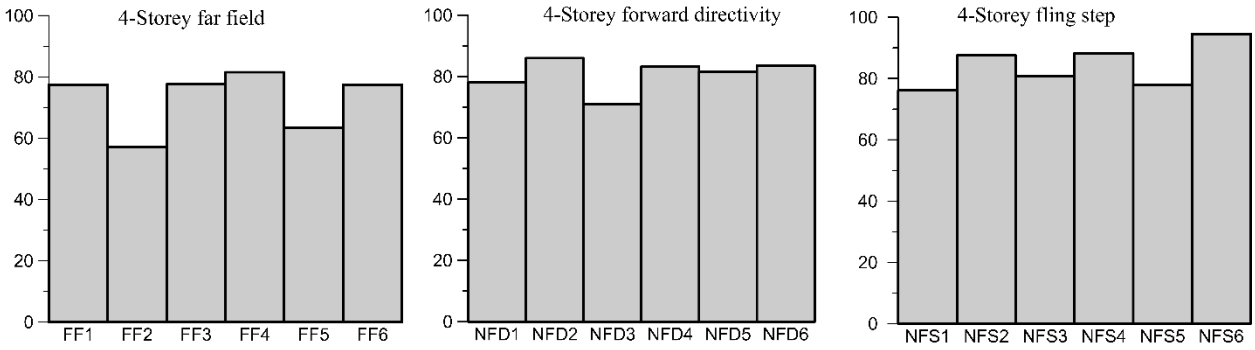

Figure 7. *Four storey base shear ratio of fixed base vs base-isolated structure of NLTHA*

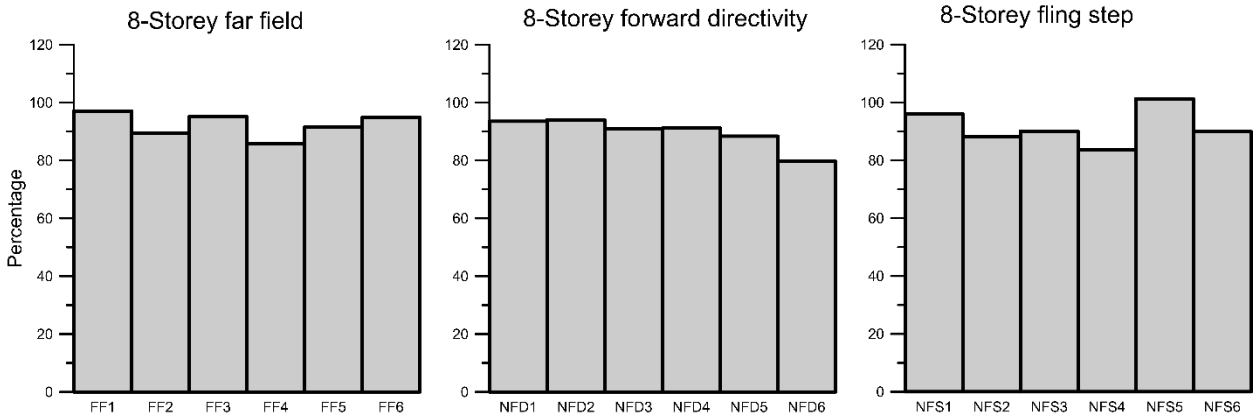

Figure 8*. Eight storey base shear ratio of fixed base vs base-isolated structure of NLTHA*

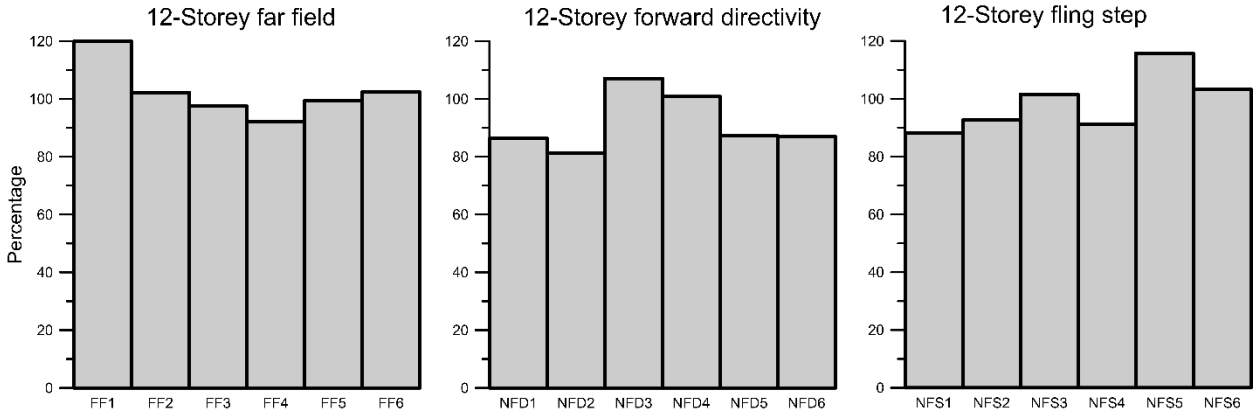

Figure 9. *Twelve storey base shear ratio of fixed base vs base-isolated structure of NLTHA*

6. DISCUSSION OF THE RESULTS

As observed in Tables 4 -7, the horizontal stiffness of the seismic isolator is low, thereby the time period of a seismically isolated structure increases which in turn results in reduced base shear. The damping of the system also increases by using the isolators. Interstorey drift ratio is very much less than the convention building since the displacements are concentrated at the level of isolators. Since the floor acceleration is reduced by using the isolators, acceleration sensitive equipment in the important buildings are not much damaged.

As seen in Table 4, the difference in time period decreases with increase in height of the structure of the base-isolated structure compared to the fixed base [26]. This increases the stiffness which in turn increases the base shear in tall base-isolated structure as seen in Figures 7- 9 which also indicates that higher mode factor should be taken into account [8]. The demand parameters increase significantly for near-fault ground motion compared to far-field motion despite the lower value of peak ground acceleration of near-fault ground motion as observed from Table 5 to Table 10 for all the buildings considered [36].

The following observations are made in the study:

1. In the present procedure, $V_{b(NLTHA)}$ is within $V_{b(DDBD)}$ for both FB (fixed base) and BI (base-isolated) structure for far field ground motions (Tables 8 - 10).
2. $V_{b(NLTHA)}$ for 4-storey building exceeds $V_{b(DDBD)}$ up to 25% in near field forward directivity (NFD 1, NFD 2, NFD 4, NFD 6) and up to 20% in case of near field fling step (NFS 1, NFS 2) for the BI structure (Table 8).
3. For 8-storey BI, $V_{b(NLTHA)}$ exceeds $V_{b(DDBD)}$ up to 19% in the case of near field forward directivity (NFD 1, NFD 2) (Table 9).
4. For 12-storey BI, $V_{b(NLTHA)}$ exceeds $V_{b(DDBD)}$ up to 7% in case of near field forward directivity (NFD 2) and 31% for near field fling step (NFD 1, NFD 2) for FB structure (Table 10).
5. $V_{b(NLTHA)}$ of BI structure is greater than $V_{b(NLTHA)}$ of FB for 12-storey building as well as $V_{b(DDBD)}$ for BI is nearly equal to $V_{b(DDBD)}$ for FB (Table 10).
6. The base shear values of BI buildings in case of nonlinear time history analysis were less than the corresponding fixed support values for four storey (Figure 7) and except one case in fling step, NFS 5 in eight storey (Figure 8). But for 12 storey building exceeds the base shear values of FB (Figure 9) for the far field, near field forward directivity and near field fling step ground motions.
7. The equivalent damping in the structure with FB is the same for all the buildings since the drift limit is 2% and the plan configuration is the same (Table 4).
8. For the 4-storey building, the drift ratios of BI structure were higher in all the far field, 2 cases in forward directivity (NFD 1, NFD 4), 3 cases in fling step (NFS 1, NFS 2, NFS 4) ground motions (Table 5) when compared to FB.
9. Isolator displacement values were within the design displacement values (Tables 5 - 7).
10. There is a reduced top floor acceleration in BI buildings when compared to FB (Tables 5 - 7).
11. There is not much difference in base shear of four and eight storey fixed building, since the mode shape expression does not vary according to the height of the building as defined by Priestley et al. [8].

7. CONCLUSIONS

The Direct displacement-based design developed by Cardone et al was applied to four, eight and twelve storey buildings regular in the plan for the fixed base and lead rubber bearing as isolators, subjected to the far field, near field directivity and near field fling step ground motions. A total of eighteen ground motions, six in each type of ground motions were considered. The following conclusions were drawn from the study:

1. The method proposed by Cardone et al holds good for the far field ground motions with fixed support as well as the base-isolated buildings frames. The base shear accounts for a maximum of 76%, 76% and 64% for base-isolated buildings and 54%, 58% and 64% for fixed support four, eight and twelve storey buildings respectively.
2. The base shear demand was higher for the near field forward directivity and near field fling step method as seen by nonlinear time history analysis.
3. There was significant reduction in drift ratios in eight and twelve storey base-isolated buildings and the percentage increased for four storey although the values are very much less than the design drift of 2%. The maximum drift was predominantly in the first storey in four storey structure.
4. The reduced floor acceleration in the base-isolated building indicates the safety and comfort of the occupants.

5. Although this study proves the applicability of the method to far field ground motions, suggest that still more earthquake ground motions be considered especially for near field directivity and near field fling step method to possibly finding a modification factor.

CONFLICTS OF INTEREST

No conflict of interest was declared by the authors.

REFERENCES

[1] Shibata, A., Sozen, M. A., "Substitute-Structure Method for Seismic Design in R/C", American Society of Civil Eengineers Journal of the Structral Division, 102(1): 1–18, (1976).

[2] Applied Technology Council 40, "Seismic Evaluation and Retrofit of Concrete Buildings", (1): (1996).

[3] Federal Emergency Management Agency 273, "NEHRP guidelines for the seismic rehabilitation of buildings", (1997).

[4] Federal Emergency Management Agency 356, "Prestandard and Commentary for the Seismic Rehabilitation of Buildings", (2000).

[5] Structural Engineers Association of California, Blue Book., "Recommended Lateral Force Requirements and Commentary", (1999).

[6] Federation Internationale du Beton Bulletin 25, "Displacement-based seismic design of reinforced concrete buildings", (2003).

[7] Eurocode 8, "Design of structures for earthquake resistance —Part 1: General rules, seismic actions and rules for buildings", (July 2009): (2004).

[8] Priestley, M.J.N., Pettinga, J.D., "Dynamic Behaviour of Reinforced Concrete Frames Designed With Direct Displacement-Based Design", Journal of Earthquake Engineering, 9: 309–330, (2005).

[9] Malekpour, S., Dashti, F., "Application of the Direct Displacement Based Design Methodology for Different Types of RC Structural Systems", International Journal of Concrete Structures and Materials, 7(2): 135–153, (2013).

[10] Vidot-Vega, A.L., Kowalsky, M.J., "Drift, strain limits and ductility demands for RC moment frames designed with displacement-based and force-based design methods", Engineering Structures, 51: 128–140, (2013).

[11] Abebe, B.H., Lee, J.S., "Extension of Direct Displacement-Based Design to Include Higher Mode Effects in Planar Reinforced Concrete Frame Buildings", Journal of Earthquake Engineering Society of Korea, 22(5): 299–309, (2018).

[12] Sullivan, T.J., Lago, A., "Towards a simplified Direct DBD procedure for the seismic design of moment resisting frames with viscous dampers", Engineering Structures, 35: 140–148, (2012).

[13] Ayala, G., Castellanos, H., Lopez, S., "A displacement-based seismic design method with damage control for RC buildings", Earthquakes and Structures, 3(3): 413–434, (2012).

[14] Sheth, R., Prajapati, J., Soni, D., "Comparative study nonlinear static pushover analysis and displacement based adaptive pushover analysis method", International Journal of Structural Engineering, 9(1): 81–90, (2018).

[15] Afarani, M.H.C., Nicknam, A., "Seismic Response of Mass Irregular Steel Moment Resisting Frames (SMRF) according to performance levels from IDA approach", Gazi University Journal of Science, 25(3): 751–760, (2012).

[16] Bhandari, M., Bharti, S.D., Shrimali, M.K., Datta, T.K., "Seismic Fragility Analysis of Base-Isolated Building Frames Excited by Near- and Far-Field Earthquakes", Journal of Performance of Constructed Facilities, 33(3): 1–16, (2019).

[17] Kalkan, E., Kunnath, S.K., "Effects of fling step and forward directivity on seismic response of buildings", Earthquake Spectra, 22(2): 367–390, (2006).

[18] Moghim, F., Saadatpour, M.M., "The Applicability Of Direct Displacement-Based Design In Designing Concrete Buildings Located In Near-Fault Regions", in 14th World Conference on Earthquake Engineering, (2008).

[19] Kara, E.K., Durukan, K., "The Statistical Analysis of the Earthquake Hazard for Turkey by Generalized Linear Models", Gazi University Journal of Science, 30(4): 584–597, (2017).

[20] Sayani, P.J., Keri, L., Ryan, M., "Comparative Evaluation of Base-Isolated and Fixed-Base Buildings Using a Comprehensive Response Index", Journal of Structural Engineering, 135(June): 698–707, (2009).

[21] Bhagat, S., Wijeyewickrema, A.C., Subedi, N., "Influence of Near-Fault Ground Motions with Fling-Step and Forward-Directivity Characteristics on Seismic Response of Base-Isolated Buildings", Journal of Earthquake Engineering, 25(3): 455–474, (2021).

[22] Bhandari, M., Bharti, S.D., Shrimali, M.K., Datta, T.K., "The Numerical Study of Base-Isolated Buildings Under Near-Field and Far-Field Earthquakes", Journal of Earthquake Engineering, 22(6): 989–1007, (2018).

[23] Adnan, A., Tiong, P.L.Y., Sunaryat, J., Ghazali, M.Z.M., Malek, K.A., "Seismic base isolation of steel frame structure by hollow rubber bearings", Gazi University Journal of Science, 24(4): 841–853, (2011).

[24] Mermer, A.S., Mustafa Kaya, M., Arslan, A. S., "Using seismic isolation elements to protect cylindrical steel liquid storage tanks from destructive forces of earthquakes", Gazi University Journal of Science, 25(1): 165–173, (2012).

[25] Cardone, D., Dolce, M., Palermo, G., "Direct displacement-based design of seismically isolated bridges", Bulletin of Earthquake Engineering, 7(2): 391–410, (2009).

[26] Cardone, D., Dolce, M., Palermo, G., "Direct displacement-based design of buildings with different seismic isolation systems", Journal of Earthquake Engineering, 14(2): 163–191, (2010).

[27] Muljati, I., Kusuma, A., Hindarto, F., "Direct displacement based design on moment resisting frame with out-of-plane offset of frame", Procedia Engineering, 125: 1057–1064, (2015).

[28] IS-1893, Indian Standard Criteria for Earthquake Resistant Design of Structures-Part 1 General Provisions and Buildings. Buereau of Indian Standards, New Delhi, (2016).

[29] Mageba Bridge Products, Data Sheets "Lasto®lrb", (2012).

[30] Bridgestone Corporation, "Seicmic Isolation & Vibration Control Products Business Department", (2017).

[31] FIP Industriale, "Lead rubber bearings Series LRB", (2016).

[32] Dynamic Isolation Systems, "Seismic Isolation For Buildings and Bridges", (2007).

[33] IS-456, Indian Standard Code of Practice for Plain and Reinforced Concrete, Buereau of Indian Standards, New Delhi, (2000).

[34] Kalkan, E., Chopra, A.K., "Practical guidelines to select and scale earthquake records for nonlinear response history analysis of structures", US Geological Survey, (2010).

[35] Datta, T.K., Seismıc Analysis of Structures., John Wiley & Sons, Singapore, (2010).

[36] Sodha, A.H., Soni, D.P., Desai, M.K, Kumar, S., "Behavior of quintuple friction pendulum system under near-fault earthquakes", Journal of Earthquake and Tsunami, 11(5): 1–23, (2017).